

Bromomethylated poly(phenylene oxide) (BPPO)-assisted fabrication of UiO-66-NH₂/BPPO/polyethersulfone mixed matrix membrane for enhanced gas separation

Mingmin Jia,¹ Yi Feng,¹ Jianhao Qiu,¹ Xiaocheng Lin,² Jianfeng Yao ¹

¹College of Chemical Engineering, Jiangsu Key Lab for the Chemistry & Utilization of Agricultural and Forest Biomass, Jiangsu Key Lab of Biomass-based Green Fuels and Chemicals, Nanjing Forestry University, Nanjing 210037, China

²Laboratory of Chemical Process Intensification, College of Chemical Engineering, Fuzhou University, Fuzhou 350108, Fujian, China
Correspondence to: J. Yao (E-mail: jfyao@njfu.edu.cn)

ABSTRACT: UiO-66-NH₂ nanocrystals were synthesized and embedded into bromomethylated poly(phenylene oxide)/polyethersulfone (BPPO/PES) polymer matrix to form UiO-66-NH₂/BPPO/PES mixed matrix membranes (MMMs). The crystalline structure, interaction between UiO-66-NH₂ and BPPO, and dispersion of UiO-66-NH₂ were characterized by FTIR, XRD, and SEM. Nanoparticle dispersion was drastically enhanced with the assistance of BPPO, giving an improved adhesion between the polymer and filler particles. Owing to the intrinsic adsorption property of UiO-66-NH₂ and BPPO to CO₂, the CO₂ permeability was significantly increased. As a result, the UiO-66-NH₂/BPPO/PES membrane exhibited enhanced gas separation performance, where CO₂/N₂ and H₂/N₂ ideal selectivities were increased to 50.2 and 302.4 with a CO₂ permeability of 125.6 Barrer. © 2018 Wiley Periodicals, Inc. *J. Appl. Polym. Sci.* **2018**, *135*, 46759.

KEYWORDS: bromomethylated poly(phenylene oxide); gas separation; mixed matrix membranes; UiO-66-NH₂

Received 15 March 2018; revised 6 May 2018; accepted 18 May 2018

DOI: 10.1002/app.46759

INTRODUCTION

Membrane technology provides greater simplicity and efficiency of operation with low operating costs than traditional separation processes such as adsorption, distillation, and condensation. Owing to the ease of synthesis, polymeric membranes are cost effective and widely used for gas separation.^{1,2} However, there is a limit to the performance of polymeric membranes (the Robeson upper bound) due to the tradeoff between permeability and selectivity, the key parameters in gas separation membranes.³ To overcome this limit, mixed matrix membranes (MMMs) have been fabricated, and better gas separation performance has been achieved in such MMMs compared with pristine polymeric membranes.⁴

MMMs are usually synthesized by incorporating inorganic fillers such as zeolites,⁵ metal-organic frameworks (MOFs),^{6,7} carbon-based materials (e.g., carbon nanotubes^{8,9} and carbon molecule sieve¹⁰), and other inorganic particles (e.g., α -alumina¹¹ and clay¹²) into polymers. Among these fillers, MOFs have attracted wide attention. MOFs have a crystalline structure that is generated by linking organic ligands to metal ions. Compared to other traditional inorganic fillers, MOFs present the following

advantages: (a) the predefined dimension of the cages supply effective shortcuts for gas molecules in polymer matrix, (b) the organic character of MOF linkers can enhance the interaction between MOFs and polymers, and (c) the functionalization of the ligands of MOFs can increase the affinity of the MOFs for specific gases. Thus, all these aforementioned merits make MOFs interesting as promising fillers for MMMs in gas separation application. However, the most difficult challenge is the good dispersion of inorganic fillers and accessing defect-free MMMs. Defects are generally created because of incompatible interfaces between polymers and filler particles. Moore and Koros have summarized the different nonideal structures in MMMs, such as interface voids or sieve in a cage.¹³

MMM fabrication requires good dispersion of nanoparticles in polymer matrix. Basically, there are three ways to enhance the interfacial interaction between MOFs and polymers: (a) by choosing specific polymers with certain functional groups that can react with MOFs,¹⁴⁻¹⁶ (b) by modifying MOFs with certain functional groups such as -NH₂ or -COOH that can react with or form hydrogen bond with polymers,^{7,17-20} and (c) by adding the third agent as a coupling agent to link MOFs and polymers.^{21,22}

Additional Supporting Information may be found in the online version of this article.

© 2018 Wiley Periodicals, Inc.

Recently, Jin *et al.* fabricated MMMs by incorporating UiO-66 and UiO-66-NH₂ into polyether block amide (PEBA). With the interaction between UiO-66-NH₂ and PEBA, the UiO-66-NH₂-PEBA membrane showed higher CO₂ gas separation performance than the UiO-66-PEBA membrane (CO₂ permeability of 130 Barrer, CO₂/N₂ selectivity of 72).¹⁴ Nik *et al.* utilized amino-functionalized UiO-66 as the inorganic filler and as-synthesized polyimide (PI) as the polymeric matrix. With the formation of hydrogen bonds between polymers and fillers, the polymer membrane became much more compact and resulted in decreasing CO₂ permeability (13.7 Barrer) while increasing CO₂/N₂ selectivity (52.1).¹⁸ Besides, Coronas *et al.* synthesized UiO-66-graphene oxide (GO) and incorporated it in polyethersulfone (PES) and PI matrix. With the existence of coupling agent GO, a good filler-polymer interaction was obtained, and the permeability and selectivity were enhanced simultaneously (CO₂/CH₄ selectivity value of 51 at 21 Barrer of CO₂; H₂ permeability of 73 Barrer and H₂/CH₄ selectivity of 151).²¹

In this study, the MOF choice was UiO-66-NH₂, and the polymer choice was PES with bromomethylated poly(phenylene oxide) (BPPO) as the coupling agent. BPPO has been reported to be a new material and used to fabricate ultrafiltration membranes. Compared to other polymers such as PES, polysulfone (PS) and polyvinylidene fluoride, BPPO contains abundant reactive -CH₂Br functional groups that can easily react with -NH₂ groups.^{23,24} UiO-66-NH₂ has emerged as an efficient material for CO₂ capture and separation. Because of the presence of -NH₂ groups, UiO-66-NH₂ could react with BPPO. Considering the compatibility between BPPO and other polymers such as PES, BPPO can function as a coupling agent to link UiO-66-NH₂ and PES polymer (Figure 1) to enhance the interfacial interaction between UiO-66-NH₂ and PES. Thus, defect-free MMMs can be achieved, and enhanced gas separation performance is expected.

EXPERIMENTAL

Materials

PES (E6020P, molecular weight: 51000) purchased from BASF Company was chosen as the polymer matrix due to its excellent thermal and mechanical characteristics. BPPO was supplied by Tianwei Membrane Corporation Ltd., Shandong, China. For synthesizing UiO-66-NH₂, Zirconium(IV) chloride (ZrCl₄, 98%) was supplied from Aladdin Industrial Company, China.

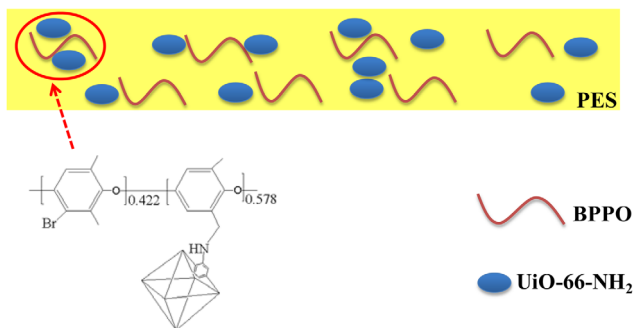


Figure 1. The schematic diagram of UiO-66-NH₂/BPPO/PES mixed matrix membrane and the interaction between UiO-66-NH₂ and BPPO. [Color figure can be viewed at wileyonlinelibrary.com]

2-Aminoterephthalic acid, *N,N*-dimethyl formamide, acetic acid, and methanol were purchased from Sinopharm Chemical Reagent Company, China. The polar and powerful solvent *N*-methyl pyrrolidone (NMP) was purchased from Sinopharm Chemical Reagent Company, China. Deionized (DI) water was used in all the experiments. All of the materials were used without further purification.

Preparation of UiO-66-NH₂ Composite Membrane

UiO-66-NH₂ was prepared by our previous work,²⁵ and well-crystallized UiO-66-NH₂ was obtained with a particle size centered at 128 nm. The MMMs were prepared by dense membrane casting method using a casting knife with a gap of 150 μ m. In the preparation of MMMs, the content of nanoparticles (fillers) was normally less than 20 wt %. For the UiO-66-NH₂/BPPO/PES MMM, the weight percent of UiO-66-NH₂ based on PES is 15 wt %. As BPPO is a kind of coupling agent, the weight ratio of BPPO/PES is 1:6. The PES was pre-dried in a vacuum oven at 110°C overnight. UiO-66-NH₂ (0.106 g) was dispersed in 7.5 g of NMP. The mixture was then stirred for 1 h and sonicated for 30 min for three cycles to obtain a homogeneous suspension. After that, 0.6 g of PES was added into the above solution and stirred until it was fully dissolved. Meanwhile, 0.1 g of BPPO was dissolved into 1 g of NMP and stirred for 3 h. Both of the UiO-66-NH₂-PES solution and BPPO solution were cooled in ice water for 3 h, mixed under stirring for 5 min, and then sonicated for 5 min at 0°C (in an ice-water bath). At such temperature, the reaction between UiO-66-NH₂ and BPPO will be slowed down. The mixed solution was cast on a clean glass plate and dried at 30°C for 24 h. The resulting membrane was denoted UiO-66-NH₂/BPPO/PES. For comparison, pristine PES membrane (0.6 g), BPPO/PES (0.1 and 0.6 g), blend membrane and UiO-66-NH₂/PES (0.15 and 0.6 g) were fabricated by a similar method as above.

Characterization

The crystalline structures of UiO-66-NH₂ and the membranes were analyzed by X-ray diffraction (XRD) using Rigaku Ultima IV with Cu K α radiation ($\lambda = 0.1542$ nm) at 40 kV at room temperature. The functional groups of the samples were characterized by Fourier transform infrared spectra (FTIR, Thermo Electron Nicolet-360, USA) using the KBr wafer technique. Morphologies of the as-prepared membranes were characterized by scanning electron microscopy (SEM) utilizing a JSM-7600F (JEOL Ltd., Japan) with an operating voltage of 5 kV. The membrane samples were prepared by cutting off the membranes with a surgical knife and subsequent sputter coating of palladium. Thermal stability of PES-based membranes was investigated using a thermogravimetric analyzer (TGA Q5000-IR, TA Instruments) from 25 to 800°C with a heating rate of 5°C/min under N₂ atmosphere.

Gas Permeability Measurement

In this study, UiO-66-NH₂ was used as the inorganic filler and BPPO as the coupling agent. Owing to the inherent adsorption capacity for CO₂ of UiO-66-NH₂ and BPPO, the CO₂ permeability performance was essential. CO₂/N₂ separation was selected as the major research subject in this study. Besides, H₂ gas separation performance was tested as the benchmark. The single gas

separation performance of membranes was measured using a flat-sheet permeability cell with an effective area of 2.84 cm² at room temperature (25°C), 0.1–0.4 MPa. Before the test, residual gas present in the membranes and the pipeline was removed by a vacuum pump. The normalized flux of the gas was measured using a bubble flow meter under constant feed pressure. Membrane permeability (P_i) can be written as

$$P_i = \frac{LN_i}{A\Delta P} \quad (1)$$

where L is the membrane thickness (cm), measured with a digital micrometer, N_i (cm³/s) is the permeate flow rate of component gas i , A (cm²) is the test area of membranes, and ΔP_i (cmHg) is the transmembrane pressure difference of i . The unit of permeability (P_i) is expressed in Barrer [1 Barrer = 10⁻¹⁰ cm³ (STP) cm/(cm² s cmHg)].

The ideal selectivity calculated from the relation between the permeabilities of the individual gases can be expressed as:

$$S_{(i/j)} = \frac{P_i}{P_j} \quad (2)$$

RESULTS AND DISCUSSION

The microstructures of dense PES membrane, BPPO, UiO-66-NH₂, BPPO/PES blend membrane, and the UiO-66-NH₂-based MMMs were analyzed by XRD. As shown in Figure 2, pristine PES and BPPO show amorphous structures with a prominent peak recorded at $2\theta = 17.5$ and 23.5°, respectively.^{12,26} By blending BPPO with PES, the peak of PES shifts from 17.5 to 18.4°. Meanwhile, the peak of BPPO is missing, indicating that BPPO is compatible with PES matrix. The XRD pattern shows that the synthesized UiO-66-NH₂ exhibits a highly crystalline structure.²⁷ For UiO-66-NH₂/PES and UiO-66-NH₂/BPPO/PES, it is clear that the UiO-66-NH₂ nanoparticles maintain their crystallinity and topology in the MMMs. Meanwhile, the peaks of UiO-66-NH₂ in PES and BPPO/PES polymers have a little decrease, suggesting that inorganic fillers were trapped in the polymer matrix.

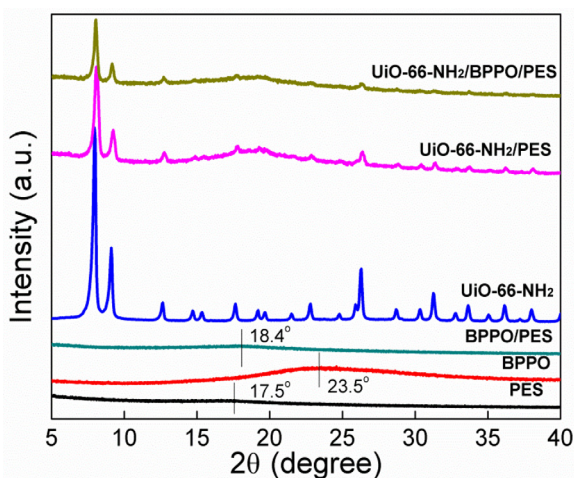


Figure 2. XRD patterns of PES membrane, BPPO, and BPPO/PES blend membrane and the UiO-66-NH₂-based mixed matrix membranes. [Color figure can be viewed at wileyonlinelibrary.com]

The morphology of as-prepared membranes was characterized by SEM. Figure 3(a,b) shows the cross-sectional SEM image of pristine PES membrane and BPPO/PES blend membrane. It can be seen that pure PES and BPPO/PES blend membrane are dense and homogeneous without any defects and voids, indicating the good compatibility between PES and BPPO. As shown in Figure 3(c), some agglomerates of UiO-66-NH₂ particles with size of some micrometers could be seen in UiO-66-NH₂/PES membrane. From the surface image [Figure 3(e)], it clearly shows that the size of agglomerated particles (170 nm) is larger than that of the original UiO-66-NH₂ nanoparticles (128 nm, as shown in Figure S1). The poor dispersion of UiO-66-NH₂ nanoparticles is attributed to the weak interaction between UiO-66 frameworks and polymer chains. Fortunately, the introduction of BPPO into the UiO-66-NH₂/PES membrane makes the UiO-66-NH₂ nanocrystals well-dispersed in the polymeric matrix. There is no aggregate of MOF particles and visible voids at the MOF–polymer interface [Figure 3(d) and Figure S2], further demonstrating the enhanced interface interaction between UiO-66-NH₂ and BPPO. Such results were quite similar to those of the PS–UiO-66-NH₂ hybrid membranes reported by Urban *et al.*²⁸ Besides, the membrane thickness was also measured using the SEM images (Figure 3), which was consistent with the results tested using the digital micrometer. From the surface image [Figure 3(f)], the size of UiO-66-NH₂ was 108 nm, which is smaller than the original size of UiO-66-NH₂ (128 nm), resulting from the well-dispersion of UiO-66-NH₂ in the polymer matrix and some UiO-66-NH₂ was extruded out of MMMs. A similar phenomenon was also observed in the work of UiO-66-NH₂-PEBA.¹⁴

To further investigate the interaction in the membranes, the FTIR spectra of pristine PES, BPPO, UiO-66-NH₂, BPPO/PES blend membrane, UiO-66-NH₂/PES, and UiO-66-NH₂/BPPO/PES MMM are presented in Figure 4. The FTIR spectrum of pristine PES membrane shows characteristic bands at around 561 (SO₂ scissors deformation), 1104 and 1153 (SO₂ symmetric stretch), 1244 (aryl–O–aryl C–O stretch), and 1294 and 1333 cm⁻¹ (SO₂ asymmetric stretch).⁹ For pristine BPPO, the characteristic peak of C–Br stretch appears at 625 cm⁻¹, and the peaks at 1610 and 1476 cm⁻¹ correspond to the phenyl group vibrations.²³ It is obvious that the characteristic peaks of BPPO almost disappear in the BPPO/PES blend membrane, which indicates that BPPO has a good compatibility with PES matrix. For UiO-66-NH₂, the striking peaks at 1662 and 1574 cm⁻¹ indicate the presence of –NH₂ groups. It is obvious that the characteristic peak of –NH₂ groups also exists in UiO-66-NH₂/PES. Besides, by incorporating UiO-66-NH₂ in PES matrix, the characteristic peak of SO₂ symmetric stretch shifts from 1153 to 1158 cm⁻¹, indicating the hydrogen bonding interaction between N–H and S=O that is called redshift as shown in Figure 4(a).¹⁴ UiO-66-NH₂/BPPO/PES membrane shows a similar FTIR spectrum to UiO-66-NH₂/PES. The interaction between –NH₂ in UiO-66-NH₂ and C–Br in BPPO was demonstrated by the direct mixture of UiO-66-NH₂ and BPPO, where the intensity of the amino characteristic peak suffers a significant reduction and the characteristic peak of C–Br stretch disappears. Meanwhile, the peak at 1383 cm⁻¹ (R₂–NH) was obviously enhanced compared with the intensity of the –

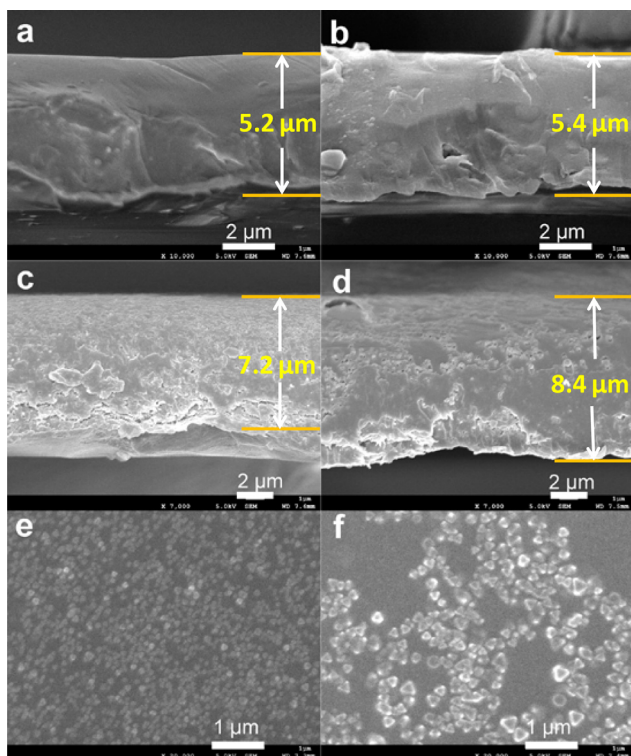


Figure 3. SEM images of (a) PES, (b) BPPO/PES, (c,e) UiO-66-NH₂/PES, and (d,f) UiO-66-NH₂/BPPO/PES membranes: cross section (a–d) and surface (e,f). [Color figure can be viewed at wileyonlinelibrary.com]

NH₂ peaks in UiO-66-NH₂@BPPO composites, indicating the interaction between the MOF and polymer [Figure 4(b)].²³

The thermal behavior and thermal decomposition were investigated to sketch the influence of the interaction between BPPO and UiO-66-NH₂ on the key properties of the UiO-66-NH₂/BPPO/PES membranes. The thermal behavior of the pristine PES, PES/BPPO, PES/UiO-66-NH₂, and UiO-66-NH₂/BPPO/PES membranes was evaluated by TGA analyses, as displayed in Figure 5(a). For pristine PES and BPPO, major weight loss occurs at 553 and 412°C, corresponding to the degradation of the polymer.^{29,30} The blend membrane (PES/BPPO) shows an obvious

weight loss up to 505°C.³¹ Meanwhile, UiO-66-NH₂ underwent an obvious weight loss below 300°C attributed to adsorbed water and other types of physical adsorption (residual DMF in the pores). The observed weight loss at high temperatures (350–600°C) corresponds to the dehydroxylation of the Zr₆O₄(OH)₄ cornerstone into Zr₆O₆.¹⁴ By incorporating UiO-66-NH₂ into PES, the degradation temperature of PES/UiO-66-NH₂ occurs at 541°C [Figure 5(b)]. In UiO-66-NH₂/BPPO/PES, UiO-66-NH₂ was incorporated into the PES/BPPO blend membrane whose degradation temperature was lower than pristine PES membrane. However, the decomposition temperature of UiO-66-NH₂/BPPO/PES (543°C) was quite close to that of PES/UiO-66-NH₂. This improvement in thermal stability may be attributed to the uniform particle dispersion and the removal of the interfacial voids.²⁹

Single-gas permeabilities across the prepared membrane are shown in Table I. For the pure PES membrane, the permeability of H₂, CO₂, and N₂ is 17.63, 6.98, and 0.60 Barrer, respectively, and the ideal selectivity of H₂/N₂ (29.4) and CO₂/N₂ (11.6) (25°C, 0.1 MPa) is in good agreement with the previous study.^{11,32} By incorporating UiO-66-NH₂ in PES matrix, the permeability for all gases shows a significant enhancement, with H₂, CO₂, and N₂ permeabilities of 161.6, 28.8, and 1.44 Barrer, respectively. This is due to the intrinsic pore size of UiO-66-NH₂ nanoparticles (0.6 nm),²⁷ which is larger than the kinetic diameters of H₂ (0.29 nm), CO₂ (0.33 nm), and N₂ (0.36 nm). Meanwhile, the CO₂-philic characteristic of UiO-66-NH₂ frameworks significantly enhanced the selectivity of UiO-66-NH₂/PES (CO₂/N₂ ideal selectivity of 20.0).¹⁴ In the BPPO/PES blend membrane, the permeability of N₂ (0.76 Barrer) and H₂ (25.23 Barrer) was increased a little.^{33,34} Besides, on account of the inherent preferential adsorption of BPPO for CO₂, the permeability of CO₂ was increased (12.56 Barrer) by 80%, as compared to pure PES membrane. Therefore, an increased CO₂/N₂ selectivity was observed for BPPO/PES (16.5).³⁴ By introducing BPPO into the UiO-66-NH₂/PES membrane (UiO-66-NH₂/BPPO/PES), both permeability and selectivity were increased, as compared to UiO-66-NH₂/PES and BPPO/PES membranes. This should be ascribed to two reasons: (1) BPPO is well-compatible with the major polymer (PES) resulting in the good dispersion of BPPO in PES

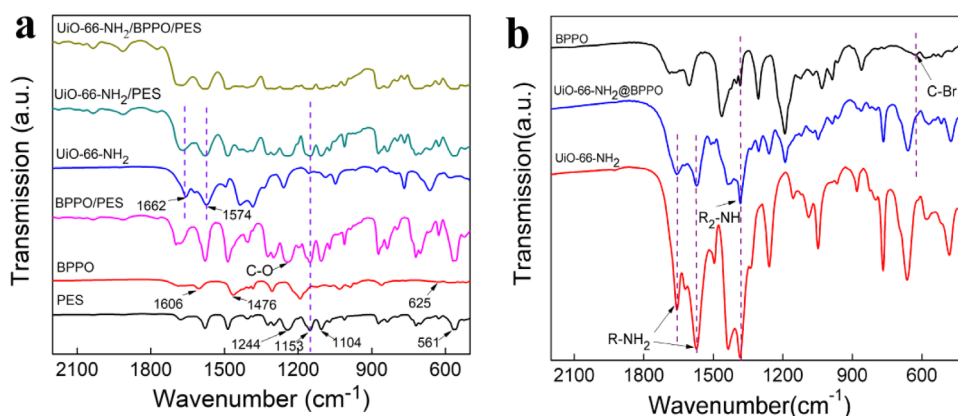


Figure 4. FTIR spectra of (a) PES, BPPO, UiO-66-NH₂, UiO-66-NH₂/PES, BPPO/PES, and UiO-66-NH₂/BPPO/PES membranes and (b) pure UiO-66-NH₂, BPPO and the mixture of UiO-66-NH₂ and BPPO (UiO-66-NH₂@BPPO). [Color figure can be viewed at wileyonlinelibrary.com]

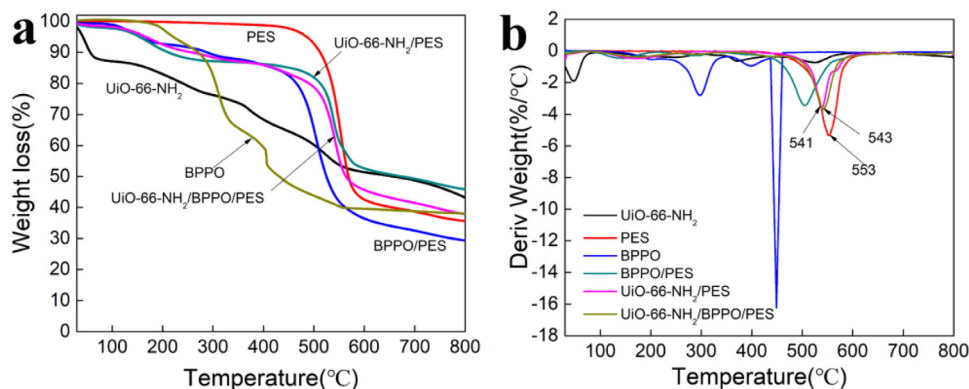


Figure 5. (a) TGA and (b) DTG thermograms of pristine PES, BPPO-PES, UiO-66-NH₂@PES, and UiO-66-NH₂@BPPO-PES membranes. [Color figure can be viewed at wileyonlinelibrary.com]

Table I. Comparison of Single Gas Permeability on Pure PES, BPPO/PES, UiO-66-NH₂/PES, and UiO-66-NH₂/BPPO/PES Membranes

Membrane	Thickness (μm)	Permeability (Barrer)			Ideal selectivity	
		N ₂	CO ₂	H ₂	CO ₂ /N ₂	H ₂ /N ₂
Pristine PES	5.2	0.60	6.98	17.63	11.6	29.4
UiO-66-NH ₂ /PES	5.4	1.44	28.77	161.6	20.0	112.2
BPPO/PES	7.2	0.76	12.56	25.23	16.5	33.2
UiO-66-NH ₂ /BPPO/PES	8.4	2.50	125.6	756.1	50.2	302.4

matrix, and (2) the close reactions between UiO-66-NH₂ and BPPO (Figure 1) well disperse UiO-66-NH₂ nanoparticles around BPPO chains within the PES matrix.²³ Therefore, the CO₂-philic property of BPPO and UiO-66-NH₂ and effective shortcuts provided by UiO-66-NH₂ significantly enhanced the permeability and selectivities, which approach the permeability/selectivity tradeoff relationship in polymeric membranes.³

The gas permeability of UiO-66-NH₂/BPPO/PES at different pressures (0.1–0.4 MPa) was also studied, as shown in Figure 6. With the increase of feed pressure, the permeability of CO₂

decreased slightly. The permeability of N₂ increased slightly, and a similar phenomenon was observed in PES-*N*-methyl-diethanolamine membrane.³⁵ As a result, the CO₂/N₂ selectivity of the UiO-66-NH₂/BPPO/PES membrane shows a decreasing trend with the increase of feed pressure. Because there is no pore in UiO-66-NH₂/BPPO/PES MMM, all gas molecules follow the solution diffusion mechanism. Owing to the inherent adsorption capacity of UiO-66-NH₂ and BPPO for CO₂, the permeability of CO₂ was enhanced compared to N₂ in 0.1 MPa. As the pressure increases, the permeability of CO₂ almost remains unchanged

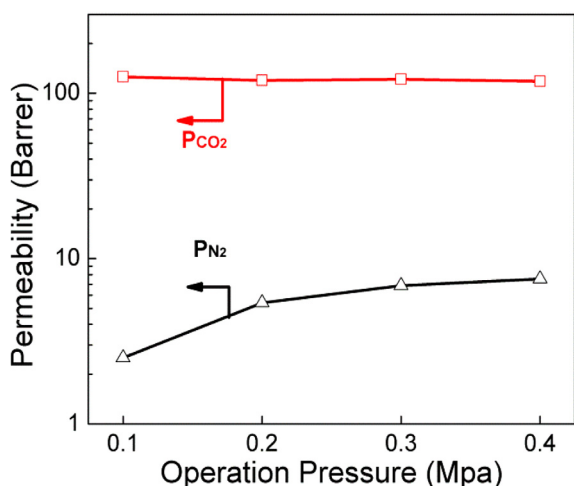


Figure 6. Effect of feed pressure on gas separation performance of membranes. [Color figure can be viewed at wileyonlinelibrary.com]

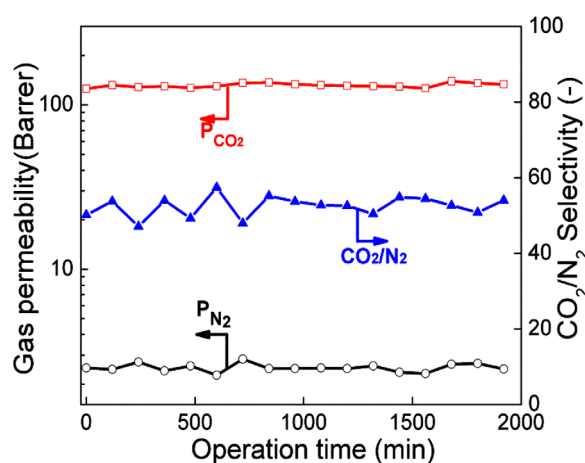


Figure 7. The operational stability of UiO-66-NH₂/BPPO/PES membrane (membranes were tested at 0.1 MPa, 25°C). [Color figure can be viewed at wileyonlinelibrary.com]

Table II. Comparison of Gas Permeability Results of PES-Based MMMs Embedded with Different Types of Filler

Filler	Testing conditions		Permeability (Barrer) Selectivity						References
	P (bar)	T (°C)	N ₂	CO ₂	H ₂	CH ₄	CO ₂ /N ₂	CO ₂ /CH ₄	
Zeolite 4A	10	35	0.066	1.3	4.3	0.030	19.7	43.3	17
Zeolite 5A	10	35	0.085	2.5	11	0.065	29.4	38.5	
MWCNTs	3(N ₂); 4(CO ₂ , CH ₄)	27	5.35	45.3	-	2.33	8.46	19.6	37
α-Alumina	4	25	0.45	6.4	59	-	14.2	-	11
SAPO-34	2	25	-	453.0	-	37.4	-	12.1	38
Cloisite15A	3	25	-	2.8	-	0.06	-	46.7	12
SAPO-34 (HMA)	2	35	-	2.38	9.35	0.0074	-	33.1	32
SAPO-34 (Tf ₂ N)	30	25	-	21 000	-	335.3	-	62.6	39
CMS (DEA)	6	25	-	9170.8	-	178.4	-	51.4	10
UiO-66-NH ₂	1	25	1.44	28.7	161.6	-	20.0	-	This work
UiO-66-NH ₂ (BPPO)	1	25	2.5	125.6	756.1	-	50.2	-	This work

P in Barrer [1 Barrer = 1×10^{-10} cm³ cm/(cm² s cm Hg)].

because of the adsorption site saturation. However, the permeability of N₂ gas molecules through the membrane only follows the solution diffusion mechanism without any adsorption facilitation. With the increase of the N₂ concentration on the membrane surface, the permeability increases a little.³⁶

The stability of the membrane is a vital characteristic that determines the viability for practical applications. As shown in Figure 7, the stability of UiO-66-NH₂/BPPO/PES membrane is tested up to 2000 min under the CO₂ and N₂ single gas at 25°C and a feed pressure of 0.1 MPa. Despite a little fluctuation, the curves of the CO₂ and N₂ permeability and the CO₂/N₂ selectivity are broadly stable throughout the test. These results demonstrate the good stability of the UiO-66-NH₂/BPPO/PES membrane.³⁶

Table II shows the comparison of gas separation performance for the PES-based MMMs with other types of fillers in the literature.

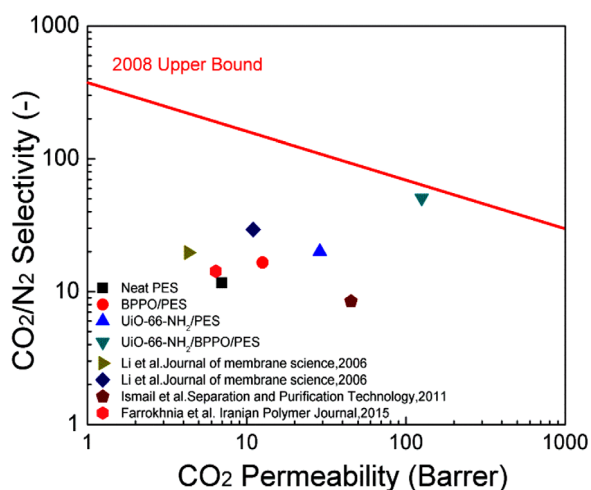


Figure 8. Comparison of CO₂/N₂ separation for pristine PES, BPPO/PES, UiO-66-NH₂/PES, UiO-66-NH₂/BPPO/PES, and a series of PES-based membranes with Robeson upper bound. [Color figure can be viewed at wileyonlinelibrary.com]

We determined the gas transport results of a series of MMMs upon the addition of different fillers. Besides, the comparison with the Robeson upper bound is shown in Figure 8. Compared with pure PES membrane, both BPPO/PES blend membrane and UiO-66-NH₂/PES MMMs exhibit improved CO₂/N₂ gas separation performance. However, it can be obviously found that the UiO-66-NH₂/BPPO/PES MMM shows higher CO₂ permeability and selectivity than BPPO/PES blend membrane and UiO-66-NH₂/PES MMMs. Furthermore, UiO-66-NH₂/BPPO/PES MMM approaches the upper bound for state-of-the-art membranes. This endows the developed UiO-66-NH₂ MOFs MMMs with potentiality for practical application.

CONCLUSIONS

In summary, we reported the design and fabrication of BPPO-assisted UiO-66-NH₂/BPPO/PES MMMs. By incorporating BPPO as the coupling agent, UiO-66-NH₂/BPPO/PES MMM showed an enhanced morphology and thermal stability as revealed by SEM and TGA, resulting from the interaction between UiO-66-NH₂ and BPPO. Meanwhile, UiO-66-NH₂ in polymer matrix provided shortcuts for gases, and the permeability of MMMs was enhanced. Furthermore, owing to the intrinsic adsorption of CO₂ on UiO-66-NH₂ and BPPO, the CO₂ permeability was significantly enhanced. The as-prepared UiO-66-NH₂/BPPO/PES exhibited high and stable CO₂/N₂ separation performance, with H₂, CO₂, and N₂ permeabilities of 756.1, 125.6, 2.5 Barrer, respectively (CO₂/N₂ ideal selectivity of 50.2 and H₂/N₂ ideal selectivity of 302.4).

ACKNOWLEDGMENTS

The authors are grateful for the financial support of Natural Science Key Project of the Jiangsu Higher Education Institutions (15KJA220001), Jiangsu Specially-Appointed Professor Program (JSAPP201411), Young Natural Science Foundation of Jiangsu Province (BK20170919), and Priority Academic Program Development of Jiangsu Higher Education Institutions (PAPD).

REFERENCES

1. Yao, J. F.; Wang, H. T. *Chem. Soc. Rev.* **2014**, *43*, 4470.
2. Yao, J.; Dong, D.; Li, D.; He, L.; Xu, G.; Wang, H. *Chem. Commun.* **2011**, *47*, 2559.
3. Robeson, L. M. *J. Membr. Sci.* **2008**, *320*, 390.
4. Chung, T.-S.; Jiang, L. Y.; Li, Y.; Kulprathipanja, S. *Prog. Polym. Sci.* **2007**, *32*, 483.
5. Yong, H. H.; Park, N. C.; Kang, Y. S.; Won, J.; Kim, W. N. *J. Membr. Sci.* **2001**, *188*, 151.
6. Perez, E. V.; Balkus, K. J.; Ferraris, J. P.; Musselman, I. H. *J. Membr. Sci.* **2009**, *328*, 165.
7. Venna, S. R.; Lartey, M.; Li, T.; Spore, A.; Kumar, S.; Nulwala, H. B.; Luebke, D. R.; Rosi, N. L.; Albenze, E. *J. Mater. Chem. A.* **2015**, *3*, 5014.
8. Ge, L.; Zhu, Z.; Li, F.; Liu, S.; Wang, L.; Tang, X.; Rudolph, V. *J. Phys. Chem. C.* **2011**, *115*, 6661.
9. Ge, L.; Zhu, Z.; Rudolph, V. *Sep. Purif. Technol.* **2011**, *78*, 76.
10. Nasir, R.; Mukhtar, H.; Man, Z.; Shaharun, M. S.; Abu Bakar, M. Z. *RSC Adv.* **2015**, *5*, 60814.
11. Farrokhnia, M.; Rashidzadeh, M.; Safekordi, A.; Khanbabaie, G. *Iran. Polym. J.* **2015**, *24*, 171.
12. Ismail, N. M.; Ismail, A. F.; Mustafa, A.; Zulhairun, A. K.; Nordin, N. A. H. M. *J. Polym. Eng.* **2016**, *36*, 65.
13. Moore, T. T.; Koros, W. J. *J. Mol. Struct.* **2005**, *739*, 87.
14. Shen, J.; Liu, G.; Huang, K.; Li, Q.; Guan, K.; Li, Y.; Jin, W. *J. Membr. Sci.* **2016**, *513*, 155.
15. Xiang, L.; Sheng, L.; Wang, C.; Zhang, L.; Pan, Y.; Li, Y. *Adv. Mater.* **2017**, *29*, 1606999.
16. Wang, Z.; Wang, D.; Zhang, S.; Hu, L.; Jin, J. *Adv. Mater.* **2016**, *28*, 3399.
17. Li, Y.; Guan, H. M.; Chung, T. S.; Kulprathipanja, S. *J. Membr. Sci.* **2006**, *275*, 17.
18. Nik, O. G.; Chen, X. Y.; Kaliaguine, S. *J. Membr. Sci.* **2012**, *413*, 48.
19. Jia, M.; Feng, Y.; Liu, S.; Qiu, J.; Yao, J. *J. Membr. Sci.* **2017**, *539*, 172.
20. Mustafa, S. G. E. E.; Mannan, H. A.; Nasir, R.; Mohshim, D. F.; Mukhtar, H. *J. Appl. Polym. Sci.* **2017**, *134*, 45345.
21. Castarlenas, S.; Tellez, C.; Coronas, J. *J. Membr. Sci.* **2017**, *526*, 205.
22. Lin, R. J.; Ge, L.; Hou, L.; Strounina, E.; Rudolph, V.; Zhu, Z. H. *ACS Appl. Mater. Inter.* **2014**, *6*, 5609.
23. Feng, Y.; Lin, X. C.; Li, H. Z.; He, L. Z.; Sridhar, T.; Suresh, A. K.; Bellare, J.; Wang, H. T. *Ind. Eng. Chem. Res.* **2014**, *53*, 14974.
24. Fang, C.; Julius, D.; Tay, S. W.; Hong, L.; Lee, J. Y. *Polymer.* **2013**, *54*, 134.
25. Li, L.; CHung, D. D. L. *Composites.* **1992**, *25*, 215.
26. Shamsaei, E.; Low, Z.-X.; Lin, X.; Mayahi, A.; Liu, H.; Zhang, X.; Liu, J. Z.; Wang, H. *Chem. Commun.* **2015**, *51*, 11474.
27. Cavka, J. H.; Jakobsen, S.; Olsbye, U.; Guillou, N.; Lamberti, C.; Bordiga, S.; Lillerud, K. P. J. *J. Am. Chem. Soc.* **2008**, *130*, 13850.
28. Su, N. C.; Sun, D. T.; Beavers, C. M.; Britt, D. K.; Queen, W. L.; Urban, J. *J. Energy Environ. Sci.* **2016**, *9*, 922.
29. Laghaei, M.; Sadeghi, M.; Ghalei, B.; Shahrooz, M. *J. Membr. Sci.* **2016**, *513*, 20.
30. Pan, Q.; Hossain, M. M.; Yang, Z.; Wang, Y.; Wu, L.; Xu, T. *J. Membr. Sci.* **2016**, *515*, 115.
31. Mosleh, S.; Mozdianfard, M. R.; Hemmati, M.; Khanbabaie, G. *J. Polym. Res.* **2016**, *23*, 120.
32. Karatay, E.; Kalipcilar, H.; Yilmaz, L. *J. Membr. Sci.* **2010**, *364*, 75.
33. Mannan, H. A.; Mukhtar, H.; Shaharun, M. S.; Othman, M. R.; Murugesan, T. *J. Appl. Polym. Sci.* **2016**, *133*, 42946.
34. Hu, X.; Cong, H.; Shen, Y.; Radosz, M. *Ind. Eng. Chem. Res.* **2007**, *46*, 1547.
35. Nasir, R.; Mukhtar, H.; Man, Z. *J. Appl. Sci.* **2014**, *14*, 1186.
36. Wang, S.; Feng, J.; Xie, Y.; Tian, Z.; Peng, D.; Wu, H.; Jiang, Z. *J. Membr. Sci.* **2016**, *500*, 25.
37. Ismail, A. F.; Rahim, N. H.; Mustafa, A.; Matsuura, T.; Ng, B. C.; Abdullah, S.; Hashemifard, S. A. *Sep. Purif. Technol.* **2011**, *80*, 20.
38. Ahmad, N. N. R.; Mukhtar, H.; Mohshim, D. F.; Nasir, R.; Man, Z. *J. Appl. Polym. Sci.* **2016**, *133*, 43387.
39. Mohshim, D. F.; Mukhtar, H.; Man, Z. *Sep. Purif. Technol.* **2014**, *135*, 252.